Site Selectivity of Peptoids as Azobenzene Scaffold for Molecular Solar Thermal Energy Storage

Benjamin Tassignon, Zhihang Wang, Agostino Galanti, Julien de Winter, Paolo Samorì, Jérôme Cornil, Kasper Moth-poulsen, Pascal Gerbaux

Site Selectivity of Peptoids as Azobenzene Scaffold for Molecular Solar Thermal Energy Storage

Benjamin Tassignon[a,b], Zhihang Wang[c,d], Agostino Galanti[e], Julien De Winter[a], Paolo Samorì[e], Jérôme Cornil[b], Kasper Moth-Poulsen[c,f,g,h], Pascal Gerbaux[a*].

[a] B. Tassignon, Dr. J. De Winter and Prof. P. Gerbaux
Organic Synthesis and Mass Spectrometry Laboratory (S²MOs), Chemistry Department, Research Institute for Biosciences
University of Mons
Place du Parc 23, B-7000 Mons, Belgium
E-mail: pascal.gerbaux@umons.ac.be

[b] B. Tassignon and Prof. J. Cornil
Laboratory for Chemistry of Novel Materials, Chemistry Department, Materials Research Institute
University of Mons
Place du Parc 23, B-7000 Mons, Belgium

[c] Dr. Z. Wang, Prof. K. Moth-Poulsen
Department of Chemistry and Chemical Engineering
Chalmers University of Technology
41296 Gothenburg, Sweden

[d] Dr. Z. Wang
Department of Materials Science and Metallurgy
University of Cambridge
27 Charles Babbage Rd, Cambridge, CB3 0FS, UK

[e] Dr. A. Galanti and Prof. P. Samorì
Institut de Chimie Supramoléculaire (ISIS), CNRS
University of Strasbourg
67000 Strasbourg, France

[f] Prof. K. Moth-Poulsen
The Institute of Materials Science of Barcelona
ICMAB-CSIC
Bellaterra, 08193 Barcelona, Spain

[g] Prof. K. Moth-Poulsen
Catalan Institution for Research & Advanced Studies
ICREA
Pg. Lluís Companys 23, 08010 Barcelona, Spain

[h] Prof. K. Moth-Poulsen
Department of Chemical Engineering
Universitat Politècnica de Catalunya, EEBE
Eduard Maristany 10–14, 08019 Barcelona, Spain

Abstract:

Storing solar energy is a key challenge in modern science. MOlecular Solar Thermal (MOST) systems, in particular those based on azobenzene switches, have received great interest in the last decades. The energy storage properties of azobenzene ($t_{1/2}$ < 4 days; ΔH~270 kJ/kg) must be improved for future applications. Herein, we introduce peptoids as programmable supramolecular scaffolds to improve the energy storage properties of azobenzene-based MOST systems. We demonstrate with 3-unit peptoids bearing a single azobenzene chromophore that dynamics of the MOST systems can be tuned depending on the anchoring position of the photochromic unit on the macromolecular backbone. We measured a remarkable increase of the half-life of the metastable form up to 14 days at 20 °C for a specific anchoring site, significantly higher than the isolated azobenzene moiety, thus opening new perspectives for MOST development. We also highlight that liquid chromatography coupled to

mass spectrometry does not only enable to monitor the different stereoisomers during the photoisomerization process as traditionally done, but also allows to determine the thermal back-isomerization kinetics.

Introduction

The grand scientific and technological challenge of thermal storage of solar energy has been pursued so far by mastering different strategies. The simplest one probably relies on the use of hot water or molten salts, which however suffers from the fact that the storage medium must be kept well insulated to avoid thermal losses [1,2]. Molecules that are capable to undergo light-induced isomerization to a metastable isomer can be used to store solar energy as chemical energy. Such systems are nowadays known as **MO**lecular **S**olar **T**hermal systems (MOST) [2–4]. The exposure of these compounds to sunlight generates a higher energy photoisomer whose storage half-life is considered as one of the principal criteria for storage purpose. When energy is needed, the photoisomer can be converted back to the stable compound upon activation such as heating or catalysis, releasing the excess energy under the form of heat [3–5].

Among the molecular solar thermal systems, azobenzene is a commonly used molecular switch. Azobenzene (**AB**) $E \rightarrow Z$ photoisomerization [6–8] has been the subject of an extensive research effort aimed at reaching optimal performances by: (i) maximizing the energy storage density (expressed in kJ/kg), that is related to the ΔH of the isomerization reaction and molecular weight, (ii) optimizing the overlap between the solar spectrum and absorption profile of the lowest energy isomer, (iii) limiting the overlap between the absorption spectra of both isomers to shift the photostationary state (PSS) toward the products; (iv) optimizing the quantum yield of photoconversion, and (v) optimizing the cyclability of the systems. Another critical parameter is the half-life ($t_{1/2}$) of the metastable isomer in storage conditions. This $t_{1/2}$ is related to the activation energy (E_a) of the thermal back isomerization and recent studies endeavor to maximize it to guarantee a long storage period [7,9–14].

AB absorbs light in the UV-vis and releases heat upon back isomerization from *Z* to *E*. The typical absorption spectrum of unsubstituted **AB** in the *E* form consists of two well separated bands: a strong π-π* transition at ~320 nm and a weaker n-π* transition at ~450 nm. For the *Z*-isomer, the strong π-π* transition is observed at ~270 nm, whereas a more intense n-π* transition compared to the *E* isomer is still present at ~450 nm, resulting in an overlap between the absorption spectra of both isomers [8,15,16]. The MOST characteristics of **AB** can be significantly improved upon substitution, typically via push-pull systems, by increasing the endothermicity of the $E \rightarrow Z$ isomerization and inducing a significant bathochromic effect to its π-π* absorption band. However, these **AB** derivatives are most of the time characterized by short *Z* isomer half-life ($t_{1/2}$), ranging from seconds to days depending on the position and electronic properties of the substituents [17]. Solvent-free liquids have also been explored to avoid both detrimental solvent effects on the isomerization mechanism and dilution of the chromophore. For azobenzene derivatives, this is for instance done by introducing long branched alkyl chains on their backbone at the expense of the energy density due to the molecular weight increase [18]. Another strategy to increase the azobenzene MOST performance in solvent-free environments is based on combining photoisomerization and phase transfer, as increasingly explored using photochromic dendrimers [19], microphase separation of block copolymers [20] and supramolecular cation-π interactions [21]. Anchoring **AB** onto carbon nanotubes (CNTs) was also envisaged to create a close-packed ordered arrangement of photoresponsive molecules whose intermolecular interactions were theoretically shown to increase the storage energy per **AB** molecule by up to 30% compared

to the single molecule [10,22]. However, to date the developed hybrid materials display a too low packing density to exhibit such enhanced properties [23]. The incorporation of **AB** moieties as side chains all along synthetic polymer backbones has been further proposed by Zhitomirsky *et al.* using a radical polymerization of an **AB**-modified acrylate monomer, though with limited success in terms of the energy stored ΔH, probably due to the rather high flexibility of the polyacrylate backbone [24].

In this context, peptoids combined with an **AB**-type molecular switch appear as a very attractive platform for molecular solar thermal systems for multiple reasons. Peptoids consist of sequence-defined synthetic polyamides with an achiral backbone which can be decorated with diverse side chains at specific positions [20]-[21]. Peptoids belong to the foldamer family, implying that they can adopt specific stable secondary structures in solution by selection of appropriate side chains [27–30]. The manipulation of their secondary structures also allows to finely tune their intermolecular interactions [31,32]. Short sequence-defined peptoids are typically synthesized using an on-resin solid support protocol developed by Zuckermann *et al.*, allowing for a precise control of sequence and size due to the step-by-step procedure [33,34]. The chemical nature of the peptoid backbone also represents an advantage for cyclability of the MOST system due to the chemical stability of the amide bonds [31,35]. In addition, the skeleton of the peptoid contributes little to the molecular mass of the macromolecule and is thus prone to maximize its energy density. Peptoids with a single **AB** moiety were prepared by Shah *et al.* in the context of developing photoresponsive peptoid oligomers [36]. In this study, the authors suggested that the kinetic stability of the thermally less stable *cis*-azobenzene side chain could be significantly enhanced by elongating the peptoid oligomer beyond the trimer length [36]; however, they did not investigate the influence of the position of the azobenzene residue within the peptoid trimer on the half-lives of the *Z*-isomers.

In this study, we demonstrate that the position of the **AB** anchoring site on a three-unit peptoid backbone, i.e. external (N and C terminus) vs internal positions, has a huge impact on the MOST properties, in particular on the metastable isomer half-life. Such a site selectivity will certainly prove to be of prime interest for the design of specific architectures to meet the requirements of the targeted applications.

Liquid Chromatography-Mass Spectrometry (LC-MS) is routinely used to characterize the relative population of the isomers of photoswitches in various fields, such as photopharmacology [37] and materials science [38]. We will go one step further here by relying on LC-MS experiments to determine the kinetics of the thermal back isomerization process by repeating LC-MS measurements at several time delays while conserving the irradiated peptoid solutions in the HPLC autosampler, in the dark at controlled temperature.

Results and Discussion

Three-unit peptoids were prepared with isomeric sequences, namely N*azb*N*spe*N*spe*, N*spe*N*azb*N*spe*, and N*spe*N*spe*N*azb* (**Scheme 1**), presenting the chromophore at different positions, *i.e.* N terminus (**N_{ter}-azo**), central (**center-azo**) and C terminus (**C_{ter}-azo**) positions, respectively. The (S)-1-phenylethyl side chain - N*spe* - has been selected due to its propensity to generate helical structure upon chain elongation (n>5) for future investigations [29,30,39]. Note that, for the **C_{ter}-azo** and **center-azo**, the azo-substituted nitrogen atoms are amide nitrogen atoms, whereas the N_{ter} nitrogen atom is a secondary amine function. The peptoids have been purified by flash chromatography and characterized by mass spectrometry (including tandem mass spectrometry analysis, see SI).

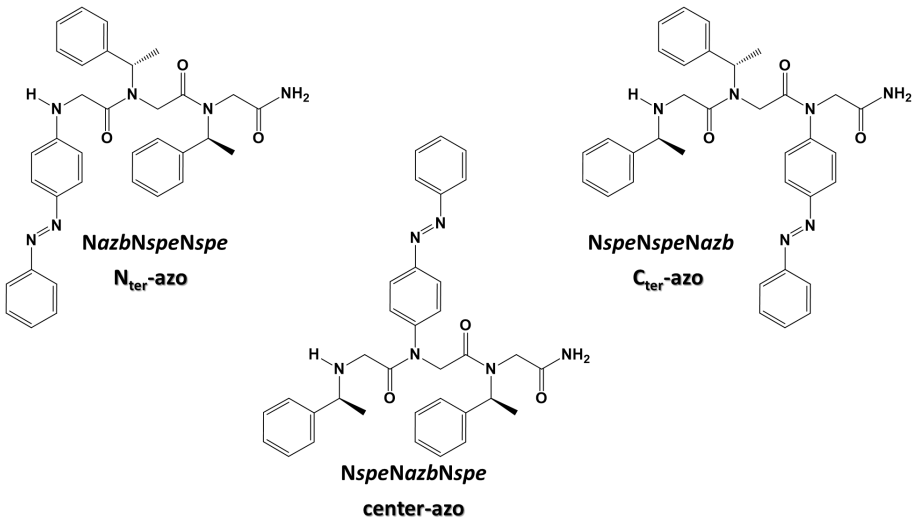

Scheme 1. Chemical formula of the three-unit peptoids with Nazb as chromophore and Nspe as helix inducer. Note the different nature of the nitrogen atoms bearing the azobenzene chromophores, amide versus amine nitrogen atoms for center-azo / C_{ter}-azo and N_{ter}-azo, respectively.

Figure 1 displays the UV-vis spectra of the three-unit peptoids recorded in the dark at room temperature in methanol, see also **Table 1**. It reveals that globally the UV-vis absorbance of **center-azo** and **C$_{ter}$-azo** are highly similar and characteristic of the presence of the azobenzene chromophore, with well-resolved π-π* (intense UV band – 325 nm) and n-π* (small visible band – 440 nm) transitions [6,16]. However, the molar extinction coefficients of the π-π* band determined as 1.8 10^4 and 2.3 10^4 $L \cdot mol^{-1} \cdot cm^{-1}$ for **center-azo** and **C$_{ter}$-azo,** respectively (see SI and **Table 1**) evidence a mild difference, revealing an impact of the incorporation of azobenzene at the central position of the peptoid on its absorptivity (for comparison, the ε of unsubstituted **AB** π-π* band is equal to ~2.2 10^4 $L \cdot mol^{-1} \cdot cm^{-1}$ in methanol [15]). For the **N$_{ter}$-azo** isomer, the π-π* transition (391 nm) overlaps the n-π* band due to a 65 nm bathochromic shift and is characterized by a molar extinction coefficient at 2.1 10^4 $L \cdot mol^{-1} \cdot cm^{-1}$. The UV-vis data of the three peptoids are consistent with the spectroscopic properties of aminoazobenzene and *N*-acetylaminoazobenzene [8,15,23].

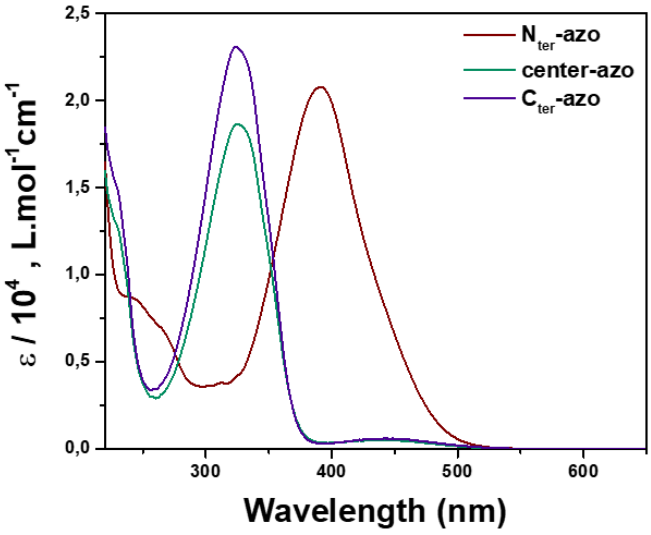

Figure 1. UV-vis spectra of the three-unit peptoids (C = 5.10^{-5} M - MeOH).

Upon continuous irradiation at 365 nm in methanol (see SI), the $E \rightarrow Z$ photoisomerization of both **center-azo** and **C_{ter}-azo** was clearly detected using UV-vis spectroscopy, as featured in **Figure 2** and SI (**Figure S11**). The observed hypsochromic shift of the π-π* band and the increase of the n-π* band absorbance are typical of the $E \rightarrow Z$ azobenzene photoisomerization [8,40], thus implying that the peptoid backbone does not preclude the chromophore isomerization, coherently with the data reported by Shah *et al.* for the **center-azo** peptoid [36]. From the PSS, the methanolic solutions were subsequently irradiated with 455 nm light (*i.e.* targeting the n-π* absorption band) to trigger the photochemical $Z \rightarrow E$ back-isomerization, as successfully monitored using UV-vis spectroscopy for both **center-azo** (**Figure 2**) and **C_{ter}-azo** (see SI, **Figure S11**) peptoids. The cyclability of the $E \rightarrow Z$ and $Z \rightarrow E$ photoisomerization process has been evaluated for **center-azo** and no significant loss in absorbance at 325 nm has been detected on ten consecutive 365/455 nm irradiation cycles, see SI. This is promising, as it shows the robustness and applicability of the photoswitch as MOST system.

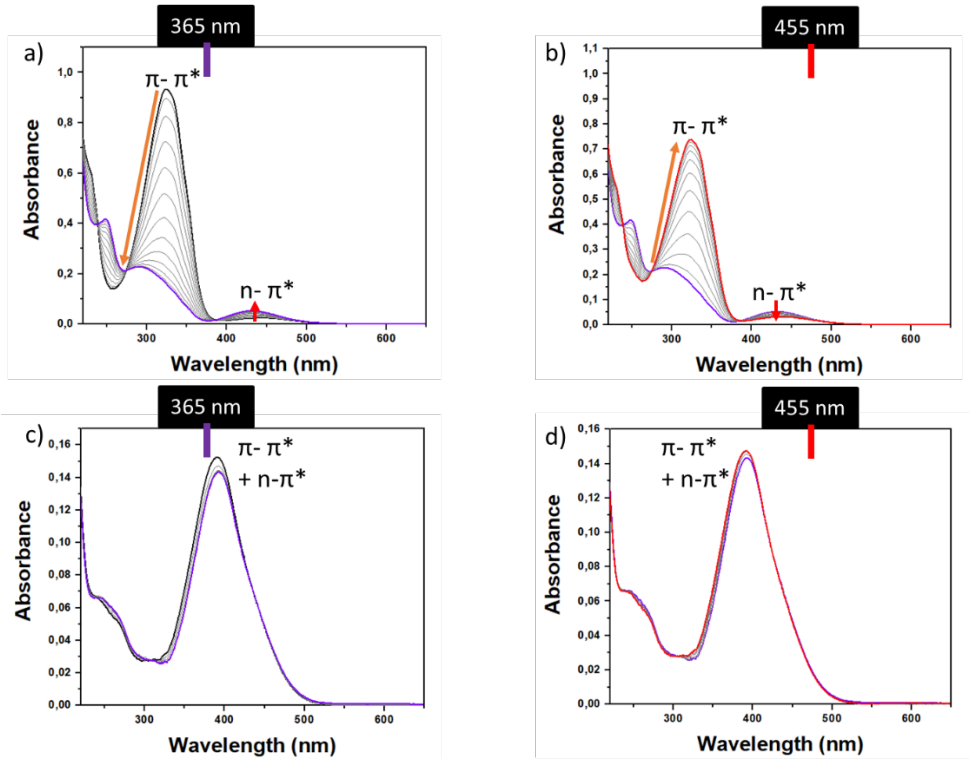

Figure 2. Photoisomerization of the azobenzene-containing peptoids monitored by UV-Vis spectroscopy: a) 365 nm irradiation of center-azo (MeOH, 5.0 10^{-5} M); b) 455 nm irradiation of center-azo from the PSS (MeOH, 5.0 10^{-5} M); c) 365 nm irradiation of N_{ter}-azo (MeOH, 8.5 10^{-6} M); and d) 455 nm irradiation of N_{ter}-azo from the PSS (MeOH, 8.5 10^{-6} M) : black line, no irradiation; purple line, UV-PSS; red line, vis-PSS.

On the other hand, little evidence of the photoisomerization of the **N_{ter}-azo** peptoid has been obtained by UV-vis spectroscopy, as only small variations were visible upon continuous irradiation at both 365 and 455 nm, see **Figure 2**. Positioning **AB** on the amino nitrogen atom at the Nter of the **N_{ter}-azo** peptoid thus appears to strongly increase the thermal $Z \rightarrow E$ back-isomerization rate of the azobenzene chromophore, as already demonstrated for 4-aminoazobenzene chromophores [8], making this peptoid not suitable for solar energy storage applications.

Monitoring the photoisomerization and back isomerization processes for azobenzene chromophores by UV-vis spectroscopy is complicated due to the overlapping of the UV-vis spectra of both stereoisomers [3,4]. We thus implemented an LC-MS based method for

monitoring both processes, including the determination of the PSD (Photostationary state distribution) and the kinetics parameters (*e.g.* $t_{1/2}$ at different temperatures) of the thermal back isomerization. Note that, to the best of our knowledge, LC-MS experiments have never been exploited for the determination of the kinetic parameters (enthalpy and entropy of activation) of the thermal back isomerization reaction. **Figure 3** clearly demonstrates that LC-MS experiments are efficient to monitor the photo- and thermal back-isomerization processes undergone by the **center-azo** and **C_{ter}-azo** peptoids.

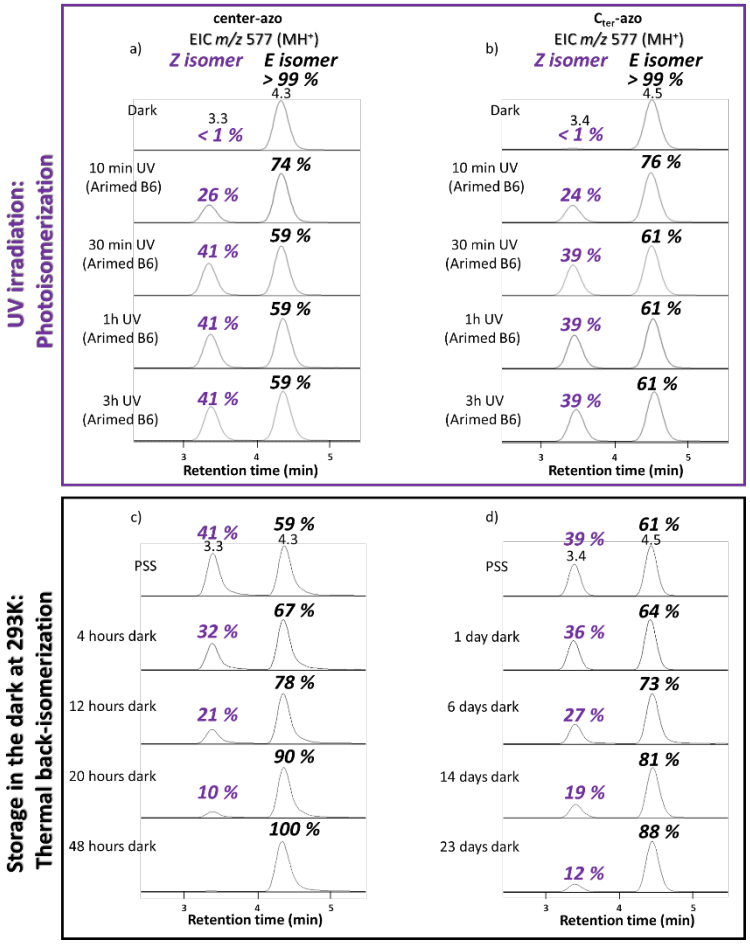

Figure 3. LC-MS analysis (Extracted Ion Current (EIC) chromatograms of the $[M+H]^+$ ions at m/z 577) of the photoisomerization and thermal back isomerization processes. Overtime evolution of the relative proportions of the center-azo peptoid steroisomers (a) under continuous irradiation using a UV Arimed B6 lamp and (c) during storage in the dark at 293 K from the UV photostationary state (PSS). Overtime evolution of the relative proportions of the C_{ter}-azo peptoid stereoisomers (b) under continuous irradiation using a UV Arimed B6 lamp and (d) during storage in the dark at 293 K from the UV photostationary state (PSS).

The UV irradiation of the peptoids was performed using an UV Arimed B6 lamp (see SI), whereas the thermal $Z \rightarrow E$ back isomerization was monitored by sampling at different times a solution of the peptoids left in the dark at a specific temperature in the HPLC autosampler (293K). We made use here of a LC chain sample manager as the dark and thermalized chamber in which the irradiated solutions were immediately stored, allowing an undisrupted LC-MS screening without any light exposure or temperature modification. From **Figure 3a** related to the **center-azo** peptoid, the PSS was shown to be reached after 30 min of irradiation, with a photostationary state composed of a mixture of 41% and 59 % of the *Z* and *E* isomers, respectively. This partial isomerization was due to the overlapping absorbance of the *E*- and *Z*-isomers. Positioning the azobenzene chromophore at the Cter did not affect significantly the

photoisomerization step, since the photostationary state was also reached in around 30 min, with a distribution of 39% and 61 % of the *Z* and *E* isomers, respectively (**Figure 3b**). Starting from the PSS, both solutions were then placed in the dark at 293 K (sample manager of the Waters Alliance 2695) and the overtime evolution of the $Z \rightarrow E$ isomer distribution was monitored by continuous sampling and LC-MS experiments. As presented in **Figure 3**, the thermal back isomerization was far slower for the **C_{ter}-azo** peptoid when compared to the **center-azo** peptoid. Indeed, 23 days were required to obtain 88% of the *E*-isomers for the **C_{ter}-azo** isomer (**Figure 3d**), whereas 90% of the *E*-isomers have been recovered after 24 hours for the **center-azo** isomer (**Figure 3c**). Based on first order kinetics, the thermal back isomerization $t_{1/2}$ were determined by exponential fitting the LC-MS data, as shown in SI; $t_{1/2}$ around 12 h and 14 days have been measured for the **center-azo** and **C_{ter}-azo** peptoids at 293K, respectively. In the literature, the $t_{1/2}$ of pristine azobenzene was reported between 2 and 4 days, depending on the experimental conditions [3,7,8]. Note also that for **center-azo**, a $t_{1/2}$ of around 6 h was measured by UV-Vis as reported by Shah *et al.* [36]. The discrepancy in the $t_{1/2}$ measurements, *i.e.* 6 h vs 12 h for the **center-azo** peptoid, probably arises from the band overlapping in UV-vis or different ionization efficiencies for both stereoisomers affecting the UV-vis and the MS data, respectively. It is worth stressing that the peptoids have been designed in the present study to avoid any difference in the stereoisomer ionization upon Electrospray, since the protonation occurs on the more basic Nter amino nitrogen atom, without affecting the azobenzene moiety.

For the **C_{ter}-azo** peptoid (longest lifetime), the $t_{1/2}$ have been further measured at different temperatures to determine the kinetics of the back reaction based on Eyring plots. Due to the volatility of the solvent, we only used four temperatures, *i.e.* 293, 303, 308 and 313K (**Figure 4**).

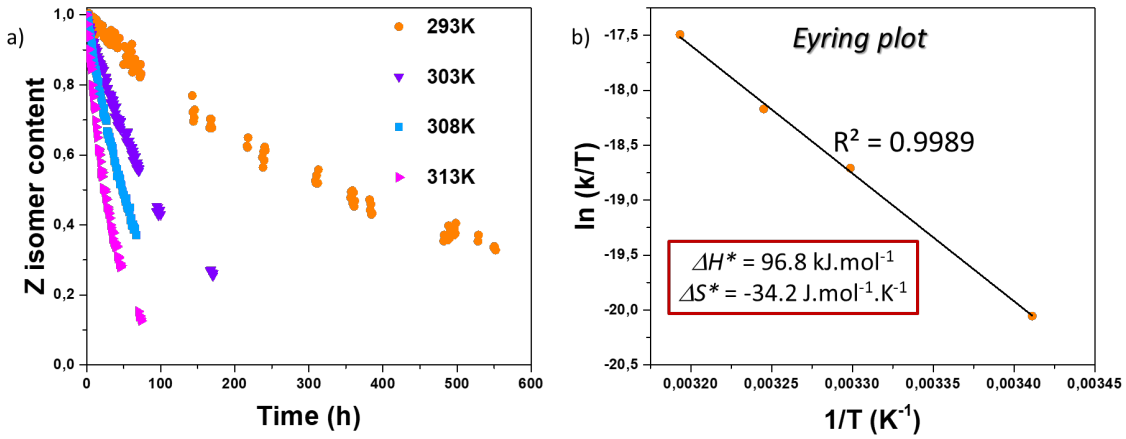

Figure 4. LC-MS monitoring of the back isomerization of the Z-isomer of the C_{ter}-azo peptoid: a) normalized plots of the Z isomer content (measured by LC-MS) as a function of the time spent in the dark at different temperatures; b) Eyring-Polanyi plot based on the rate constants extracted from the kinetics at different temperatures.

As featured in **Figure 4a**, the slight temperature increase has a strong impact on the reaction rate, since, from the PSS, 50% of the *E*-isomers of the **C_{ter}-azo** peptoids were recovered after ~1 day at 313 K *vs* 14 days at 293 K. The back isomerization kinetics parameters were then determined using the Eyring plot presented in **Figure 4b** at 96.8 kJ.mol^{-1} and -34.2 J.mol^{-1}.K^{-1} for the activation enthalpy and entropy of **C_{ter}-azo**, respectively. The entropy contribution to the activation barrier (around 10 kJ/mol at 298K) is thus much smaller than the enthalpic contribution for the back isomerization mechanism, as usually assumed for the azobenzene

MOST systems [3,7,41]. Note also that ΔH^* = 96.8 kJ.mol^{-1} was close to the value measured for pristine azobenzene (~95 kJ.mol^{-1}), revealing again the reliability and efficiency of our original LC-MS based method [3,8].

Finally, the energy stored in both the **C_{ter}-azo** and **central-azo** peptoids have been determined using DSC measurements. For the two investigated peptoids, a broad exothermic peak was observed between 70 and 120°C and corresponds to the heat released during the back-isomerization process (**Figure 5**); this allowed to determine the back isomerization enthalpies (ΔH) at 32.2 and 46.9 kJ.mol^{-1}, for the **central-azo** and **C_{ter}-azo** peptoids, respectively, to be compared with ΔH at 49 kJ.mol^{-1} for azobenzene [42]. Whereas **C_{ter}-azo** displayed a ΔH similar to pristine azobenzene, **center-azo** was characterized by a 35% loss of storage capacity which, combined to the smaller $t_{1/2}$, further demonstrates the site selectivity of the peptoid backbone allowing to tune the **AB** MOST properties. All the measured MOST properties are gathered in **Table 1**.

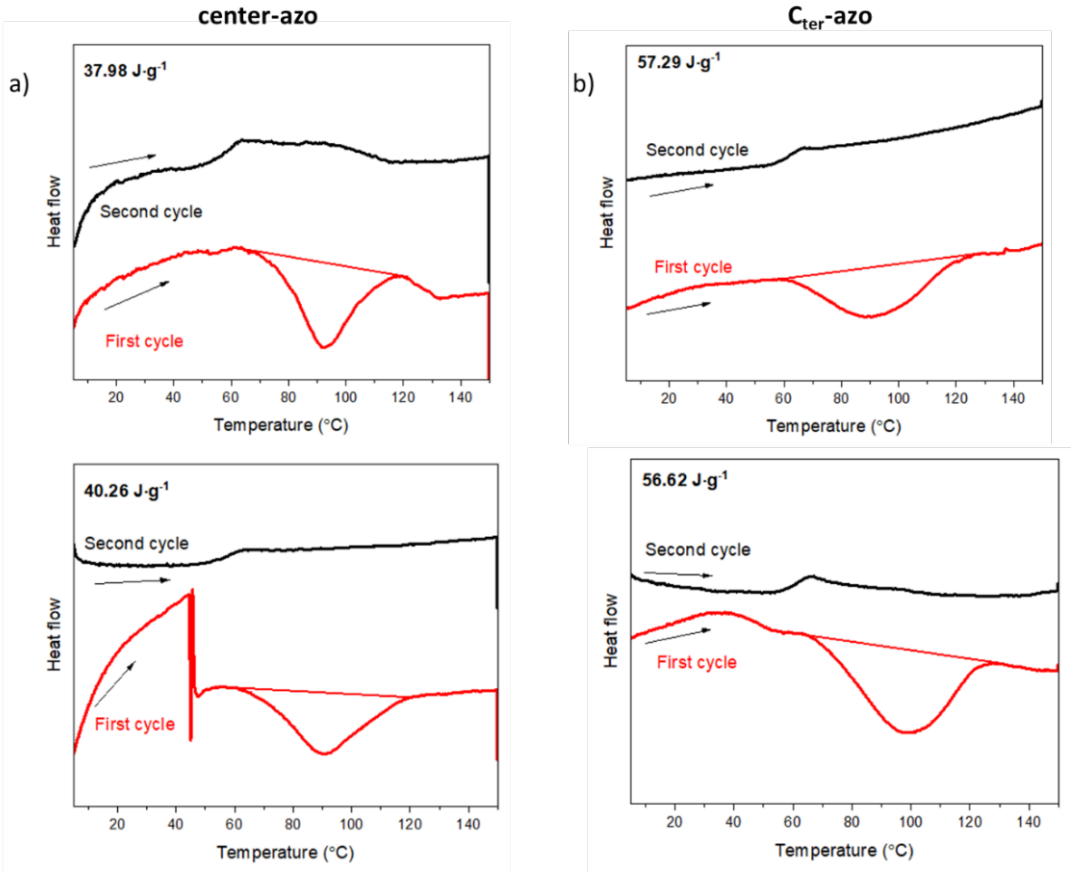

Figure 5. Differential Scanning Calorimetry (DSC) measurements for center-azo and C_{ter}-azo with the red line showing the first heating ramp and the black line the second heating ramp. a) First (up) and second (down) DSC measurements for center-azo. The signal jump observed during the first heating ramp of the second measurement was caused by instrumental fluctuation. B) First (up) and second (down) DSC measurements for C_{ter}-azo. The second cycle data allow to estimate the m.p. of the peptoids with the azobenzene chromophore in the trans-state at 70 °C.

Table 1. Relevant MOST parameters of the AB-anchored peptoids compared to pristine AB.

	$\lambda_{\pi-\pi^*}$ (nm)	$\lambda_{n-\pi^*}$ (nm)	$\varepsilon_{\lambda max}$ (10^4 L.mol^{-1}.cm^{-1})	$k_{20°C}$ (10^{-6} s^{-1})	$k_{30°C}$ (10^{-6} s^{-1})	$k_{35°C}$ (10^{-6} s^{-1})	$k_{40°C}$ (10^{-6} s^{-1})	$t_{1/2\ 20°C}$ (days)	$\Delta H^{\ddagger}$ (kJ.mol^{-1})	$\Delta H_{100\%}$ (kJ.mol^{-1})
Azobenzene	325 [a]	440 [a]	2.2 [a]	/	/	/	/	2 – 4.2 [b]	/	49 [c]
N_{ter}-azo	391	440	2.1	Too fast[d]	Too fast	Too fast	Too fast	Too fast	/	/
center-azo	325	440	1.8	15.82	/ [e]	/[e]	/[e]	0.51	/[e]	32.2
C_{ter}-azo	325	440	2.3	0.57	2.27	3.96	7.92	14.0	96.8	46.9

[a] from [12]. [b] from [3]-[7]-[8]. [c] from [3]-[36]. [d] undetected photoisomerization on the LC-MS time scale (~min). [e] not determined in the present investigation due to the short $t_{1/2}$ at 20°C.

.

Conclusion

Peptoids have been here successfully introduced as an original macromolecular programmable scaffold for tuning the properties of azobenzene (**AB**) photoswitches as MOST systems. Three-unit peptoids, equipped with a single **AB**, have been designed since they feature three different anchoring positions of the **AB**, *i.e.*, the Nter, Cter and central positions on the peptoid backbone. Our data demonstrate the high site selectivity over the MOST properties, with the metastable isomer lifetime being the most impacted characteristics. The metastable *Z* isomer could not be detected for **N_{ter}-azo**, probably due to a too short $t_{1/2}$ clearly associated with the secondary amine nature of the nitrogen atom bearing the **AB** residue. On the other hand, the **C_{ter}-azo** and **center-azo** derivatives present $t_{1/2}$ as different as 14 days and 12 hours respectively, making these positions relevant to design efficient molecular solar thermal fuels. It is worth stressing that the longest half-life of 14 days is larger than that of the isolated azobenzene unit (from 2 to 4 days), thus opening new perspectives for MOST development. Since the other MOST characteristics, *e.g.* the λ_{max}, the molar absorptivity and the storage enthalpy were only marginally affected when compared to pristine **AB**, these derivatives are not yet optimal MOST candidates, but the detected site selectivity offered by the peptoid backbone paves the way for future works, such as testing multiazobenzenic peptoids or incorporating long-lifetime arylazopyrazole chromophores [13].

To achieve such a grand-challenge, researchers will benefit from the analytical power of LC-MS experiments that proved here to be a very useful and original tool to monitor the kinetics of photo- and thermal isomerization of azobenzene photoswitches. LC-MS will become an even more informative method on peptoids containing multiple photochromic units, by allowing to identify over time the number of switched units.

Experimental Section

To define the peptoid structure, we will use the abbreviation reported in the literature. The sequence is always given from the N- to the C-terminal end, with N*azb* and N*spe* standing for the azobenzene and (S)-1-phenylethyl residues, respectively [36]-[43]-[44].

Peptoid synthesis. All reactants and solvents were commercially available (VWR Chemicals) and used without any further purification. The peptoid synthesis was performed using the on-resin solid support protocol reported by Zuckermann *et al*. which involves successive acylation and nucleophilic substitution steps [33]. The acylation step first occurs with the activation of bromoacetic acid by *N*,*N*'-diisopropylcarbodiimide, followed by the nucleophilic displacement

of bromide by a primary amine selected to incorporate the desired side chain. Both steps are repeated until the targeted sequence is obtained [33]-[34]. Primary amines used for the nucleophilic substitution steps were (S)-1-phenylethylamine and 4-aminoazobenzene. Due to the weak nucleophilicity of 4-aminoazobenzene, the reaction time for the **AB** incorporation was increased up to 16 hours and even to 24 hours (with 2 M concentration) for the C terminus position, whereas the (S)-1-phenylethylamine incorporation only required 10 minutes. Peptoids were cleaved from the resin using a 95/5 trifluoroacetic/water solution. After filtration, the acidic medium was basified to pH 10-11 using 2 M Na_2CO_3, extracted with dichloromethane and concentrated *in vacuo*. Orange powders were obtained with 70 % yield. Further purification was performed by flash column chromatography over silica gel 60 (particle size 60 – 200 µm) using dichloromethane/methanol: 96/4 as eluant.

Peptoid characterization. Peptoids were characterized by mass spectrometry (MS) by using a QToF Premier mass spectrometer (Waters, UK) equipped with an Electrospray ionization source. Primary structures and sequences were confirmed by tandem mass spectrometry (MS/MS) using B/Y, A/Y and Side Chain Loss (SCL) fragmentation patterns typical of these ions [45]-[46].

UV-vis spectroscopy UV-vis spectra were recorded from 220 to 750 nm on a Perkin Elmer Lambda 35 UV/Vis Spectrophotometer. Matched Suprasil® quartz cuvettes with 1 cm optical path length were employed for the measurements. Peptoid solutions were prepared in the dark at room temperature using HPLC grade methanol as solvent. First, spectra were recorded in the dark to prevent any photoisomerization. Molar extinction coefficients at maximum absorbance for peptoids with azobenzene in trans configuration were measured by recording the absorbance at different concentrations (ranging from 5.0 10^{-5} M to 8.6 10^{-6} M) and using the Beer-Lambert law. Irradiation was performed using 365 nm and 455 nm LEDs (Thorlabs) to study the $E \rightarrow Z$ and $Z \rightarrow E$ photochemical isomerization, respectively.

LC-MS analysis of the photoisomers Liquid Chromatography coupled to mass spectrometry analyses were performed using an Alliance 2695 HPLC (Waters, UK), equipped with an Agilent Eclipse Plus C_{18} column (4.6 x 100 mm; 3.5 µm particle size). HPLC grade solvents were used. A linear gradient starting from 70 % H_2O (with 0.01% HCOOH)/ 30 % acetonitrile going to 100 % ACN in 15 minutes was applied. Samples were dissolved in MeOH HPLC grade (1 mg mL^{-1} diluted 500x before analysis). Light irradiation to achieve $E \rightarrow Z$ photoisomerization was performed using an Arimed B6 UV lamp (Cosmedico GmbH, Stuttgart, Germany). The characteristics of the irradiation source can be found in Supporting Information (SI). Kinetics of thermal back-isomerization analyses were performed by repeating LC-MS measurements while conserving the peptoid solutions in the HPLC autosampler, *i.e.*, in the dark at controlled temperature. Both *E* and *Z* isomers were mostly detected as $[M+H]^+$ ions upon electrospray ionization in the positive ionization mode. Extracted ion current (EIC) chromatograms have been used for detecting the isomer ions and determining their relative proportions. We here assumed that the configuration of the azobenzene chromophore (*E* or *Z*) should not affect the ionization efficiency since the peptoids are systematically protonated on the N_{ter} secondary amines. For both isomers, the corresponding LC-MS ion signals including all the isotopic compositions were integrated using the integration algorithm, available under MassLynx™ 4.1 Software.

DSC measurements were performed on a Mettler Toledo DSC 2 Star system. Peptoids were irradiated at 365 nm in $CDCl_3$ until photostationary state (PSS) was reached (checked by Varian 400 MHz ^{1}H-NMR). Samples (~2 mL) were concentrated under nitrogen stream prior DSC analyses. A first heating ramp (5°C/min) was applied from 0°C to 150°C followed by a

cooling ramp and a second heating ramp to check the complete back-conversion. Energy densities were obtained by integration of the exothermic peak of the first cycle.

~~Supporting Information~~

~~The authors have cited additional references within the Supporting Information.~~ [43–46]

Acknowledgements

The UMONS MS laboratory acknowledges FRS-FNRS for the continuous support. J.C. is an FNRS research fellow. B.T. thanks the “Fonds pour la Recherche Industrielle et Agricole” for its Ph.D. grant. The S²MOs and CMN labs are grateful to the Fonds National de la Recherche Scientifique for continuing support. K.M.P and Z.W. acknowledge funding from the Swedish Research Council, The Göran Gustafson Foundation and the Swedish Energy Agency. The activity in Strasbourg has been supported by the Interdisciplinary Thematic Institute SysChem via the IdEx Unistra (ANR-10-IDEX-0002) within the program Investissement d’Avenir program, the Foundation Jean-Marie Lehn and the Institut Universitaire de France (IUF).

Keywords: azobenzene • MOST • peptoid • photoswitch • solar energy storage

References

[1] Y. Jiang, Y. Li, J. Tong, L. Mao, Y. Zhou, F. Zhang in *Molecular Devices for Solar Energy Conversion and Storage*, (Eds.: H. Tian, G. Boschloo, A.Hagfeldt), Springer, **2018**, pp 327-352.

[2] Y. Hou, R. Vidu, P. Stroeve, *Ind. Eng. Chem. Res.* **2011**, *50*, 8954–8964.

[3] T. J. Kucharski, Y. Tian, S. Akbulatov, R. Boulatov, *Energy Environ. Sci.* **2011**, *4*, 4449–4472.

[4] Z. Wang, P. Erhart, T. Li, Z. Y. Zhang, D. Sampedro, Z. Hu, H. A. Wegner, O. Brummel, J. Libuda, M. B. Nielsen, K. Moth-Poulsen, *Joule* **2021**, *5*, 3116–3136.

[5] A. Lennartson, A. Roffey, K. Moth-Poulsen, *Tetrahedron Lett.* **2015**, *56*, 1457–1465.

[6] H. Taoda, K. Hayakawa, K. Kawase, H. Yamakita, *J. Chem. Eng. Japan* **1987**, *20*, 265–270.

[7] L. Dong, Y. Feng, L. Wang, W. Feng, *Chem. Soc. Rev.* **2018**, *47*, 7339–7368.

[8] H. M. D. Bandara, S. C. Burdette, *Chem. Soc. Rev.* **2012**, *41*, 1809–1825.

[9] Y. Feng, H. Liu, W. Luo, E. Liu, N. Zhao, K. Yoshino, W. Feng, *Sci. Rep.* **2013**, *3*, 1–8.

[10] A. M. Kolpak, J. C. Grossman, *J. Chem. Phys.* **2013**, *138*, 034303.

[11] E. Durgun, J. C. Grossman, *J. Phys. Chem. Lett.* **2013**, *4*, 854–860.

[12] A. Gonzalez, M. Odaybat, M. Le, J. L. Greenfield, A. J. P. White, X. Li, M. J. Fuchter, G. G. D. Han, *J. Am. Chem. Soc.* **2022**, *144*, 19430–19436.

[13] J. Calbo, C. E. Weston, A. J. P. White, H. S. Rzepa, J. Contreras-García, M. J. Fuchter, *J. Am. Chem. Soc.* **2017**, *139*, 1261–1274.

[14] Z. Wang, H. Hölzel, K. Moth-Poulsen, *Chem. Soc. Rev.* **2022**, *51*, 7313–7326.

[15] Ľ. Vetráková, V. Ladányi, J. Al Anshori, P. Dvořák, J. Wirz, D. Heger, *Photochem. Photobiol. Sci.* **2017**, *16*, 1749–1756.

[16] J. Griffiths, *Chem. Soc. Rev.* **1972**, *1*, 481.

[17] J. Olmsted, J. Lawrence, G. G. Yee, *Sol. Energy* **1983**, *30*, 271–274.

[18] K. Masutani, M. A. Morikawa, N. Kimizuka, *Chem. Commun.* **2014**, *50*, 15803–15806.

[19] X. Xu, P. Zhang, B. Wu, Y. Xing, K. Shi, W. Fang, H. Yu, G. Wang, *ACS Appl. Mater. Interfaces* **2020**, *12*, 50135–50142.

[20] F. Cai, T. Song, B. Yang, X. Lv, L. Zhang, H. Yu, *Chem. Mater.* **2021**, *33*, 9750–9759.

[21] T. Song, H. Lei, F. Cai, Y. Kang, H. Yu, L. Zhang, *ACS Appl. Mater. Interfaces* **2022**, *14*, 1940–1949.

[22] A. M. Kolpak, J. C. Grossman, *Nano Lett.* **2011**, *11*, 3156–3162.

[23] T. J. Kucharski, N. Ferralis, A. M. Kolpak, J. O. Zheng, D. G. Nocera, J. C. Grossman, *Nat. Chem.* **2014**, *6*, 441–447.

[24] D. Zhitomirsky, E. Cho, J. C. Grossman, *Adv. Energy Mater.* **2016**, *6*, 1–8.

[25] S. B. Y. Shin, K. Kirshenbaum, *Org. Lett.* **2007**, *9*, 5003–5006.

[26] D. J. Hill, M. J. Mio, R. B. Prince, T. S. Hughes, J. S. Moore, *Chem. Rev.* **2001**, *101*, 3893–4012.

[27] C. W. Wu, T. J. Sanborn, K. Huang, R. N. Zuckermann, A. E. Barron, *J. Am. Chem. Soc.* **2001**, *123*, 6778–6784.

[28] J. R. Stringer, J. A. Crapster, I. A. Guzei, H. E. Blackwell, *J. Am. Chem. Soc.* **2011**, *133*, 15559–15567.

[29] A. S. Knight, E. Y. Zhou, M. B. Francis, R. N. Zuckermann, *Adv. Mater.* **2015**, *27*, 5665–5691.

[30] J. Seo, B.-C. Lee, R. N. Zuckermann, in *Compr. Biomater.*, Elsevier, **2011**, pp. 53–76.

[31] S. Xuan, R. N. Zuckermann, *Polymer (Guildf).* **2020**, *202*, 122691.

[32] R. J. Simon, R. S. Kania, R. N. Zuckermann, V. D. Huebner, D. A. Jewell, S. Banville, S. Ng, L. Wang, S. Rosenberg, C. K. Marlowe, D. C. Spellmeyer, R. Tan, A. D. Frankel, D. V. Santi, F. E. Cohen, P. A. Bartlett, *Proc. Natl. Acad. Sci. U. S. A.* **1992**, *89*, 9367–9371.

[33] R. Zuckermann, J. Kerr, S. Kent, W. Moos, *J. Am. Chem. Soc.* **1992**, *114*, 10646–10647.

[34] H. Tran, S. L. Gael, M. D. Connolly, R. N. Zuckermann, *J. Vis. Exp.* **2011**, 1–7.

[35] T. J. Sanborn, C. W. Wu, R. N. Zuckermann, A. E. Barron, *Biopolymers* **2002**, *63*, 12–20.

[36] N. H. Shah, K. Kirshenbaum, *Org. Biomol. Chem.* **2008**, *6*, 2516–2521.

[37] N. J. Hauwert, T. A. M. Mocking, D. Da Costa Pereira, A. J. Kooistra, L. M. Wijnen, G. C. M. Vreeker, E. W. E. Verweij, A. H. De Boer, M. J. Smit, C. De Graaf, H. F. Vischer, I. J. P. De Esch, M. Wijtmans, R. Leurs, *J. Am. Chem. Soc.* **2018**, *140*, 4232–4243.

[38] A. Galanti, J. Santoro, R. Mannancherry, Q. Duez, V. Diez-Cabanes, M. Valášek, J. De Winter, J. Cornil, P. Gerbaux, M. Mayor, P. Samorì, *J. Am. Chem. Soc.* **2019**, *141*, 9273–9283.

[39] C. W. Wu, T. J. Sanborn, R. N. Zuckermann, A. E. Barron, *J. Am. Chem. Soc.* **2001**, *123*, 2958–2963.

[40] G. Zimmerman, L. yung Chow, U. jin Paik, *J. Am. Chem. Soc.* **1958**, *80*, 3528–3531.

[41] K. Börjesson, A. Lennartson, K. Moth-Poulsen, *ACS Sustain. Chem. Eng.* **2013**, *1*, 585–590.

[42] A. W. Adamson, A. Vogler, H. Kunkely, R. Wachter, *J. Am. Chem. Soc.* **1978**, *100*, 1298–1300.

[43] S. Hoyas, E. Halin, V. Lemaur, J. De Winter, P. Gerbaux, J. Cornil, *Biomacromolecules* **2020**, *21*, 903–909.

[44] P. Weber, S. Hoyas, É. Halin, O. Coulembier, J. De Winter, J. Cornil, P. Gerbaux, *Biomacromolecules* **2022**, *23*, 1138–1147.

[45] E. Halin, S. Hoyas, V. Lemaur, J. De Winter, S. Laurent, M. D. Connolly, R. N. Zuckermann, J. Cornil, P. Gerbaux, *J. Am. Soc. Mass Spectrom.* **2019**, *30*, 2726–2740.

[46] E. Halin, S. Hoyas, V. Lemaur, J. De Winter, S. Laurent, J. Cornil, J. Roithová, P. Gerbaux, *Int. J. Mass Spectrom.* **2019**, *435*, 217–226.